High Performance Dye Sensitized Solar Cell Using Dimensionally Controlled Titania Synthesized at Sub-Zero Temperatures

Kiran P. Shejale, Devika Laishram, and Rakesh K. Sharma

Department of Chemistry, Indian Institute of Technology Jodhpur, Jodhpur, 342011, India

ESI Note S1. Raman spectroscopy analysis of anatase and rutile crystallographic phases.

Anatase TiO_2 consists of the space group I4/amd (D_{4h}^{19}) and it is assisted with two TiO_2 units in the Bravais cell. These crystals show the present lattice vibrations at the Brilliouin zone.[29]

$$\Gamma = a_{1g} + a_{2u} + 2b_{1g} + b_{2u} + 3e_g + 2e_u \quad (1)$$

The a_{1g}, $2b_{1g}$ and $3e_g$ are Raman active modes whereas the remaining three are infra-red active.[25] Rutile TiO_2 consists of the P4/mnm (D_{4h}^{14}) structure and lattice vibrations at K=0 in Brilliouin zone given as

$$\Gamma = a_{1g} + a_{2g} + a_{2u} + b_{1g} + b_{2g} + 2b_{1u} + e_g + 3e_u \quad (2)$$

The four vibrations a_{1g}, b_{1g}, b_{2g} and $3e_g$ are Raman active modes.[30]

ESI Note S2. Weight percentage calculation of rutile.

Anatase and rutile mixed phase are found in both the samples, using equation (3) weight percentage of rutile present in the prepared samples are estimated.[6]

$$WR = \frac{IR}{0.884IA + IR} \quad (3)$$

where IR and IA are diffraction peak intensities of rutile (110) and anatase (101). In the above equation, values of IR and IA are inserted for both samples and WR are calculated for both samples.

ESI Note S3. Lattice strain present on the grain boundary

To confirm this finding, the lattice strain present on the grain boundary is calculated from the XRD analysis of both samples using Williamson-Hall equation.[34]

$$\frac{\beta cos\theta}{\lambda} = \frac{1}{D} + \eta \frac{sin\theta}{\lambda} \quad (4)$$

Where, β and θ in equation (4) are full width half maximum (FWHM) and half the diffraction angle of diffraction peaks of anatase, rutile and mixed rutile-anatase phases. λ and D are the wavelength of X-ray and crystal size respectively. And η is lattice strain value. Figure S3 (Supporting information) shows linearly fitted graphs with βcosθ/λ as X axis and sinθ/λ as Y axis. The slope of the linearly fitted line is taken as effective lattice strain. This equation also represents a Uniform Deformation Model (UDM) where an assumption is made that in all the crystallographic direction uniformity of strain is present. Williamson-Hall plot of both samples with an error value also known as residual square are shown in figure S3 (Supporting information).

ESI Note S4. Dye loading

The adsorption spectra of the samples show two visible bands near 370 and 500 nm and can be described by the metal to ligand charge transfer shown in Figure S4 (supporting information). This parameter helps to measure the amount of the dye adsorbed by samples. The Beer Lambert law A = εlc was used to determine the dye loading value of the photoanode, the absorption value at 500 nm was considered. Where A is the absorbance at 500 nm, ε is the molar extinction coefficient of the N719 dye at 500 nm which is 8175/Mcm, l = 1 cm is the distance travel by light beam through solution and c is the concentration of dye adsorbed by the sample.

Figure S1. The current density – voltage curve of DSSCs where photoanode made of TiO_2 prepared at -40 °C, -30 °C, -20 °C and -10 °C.

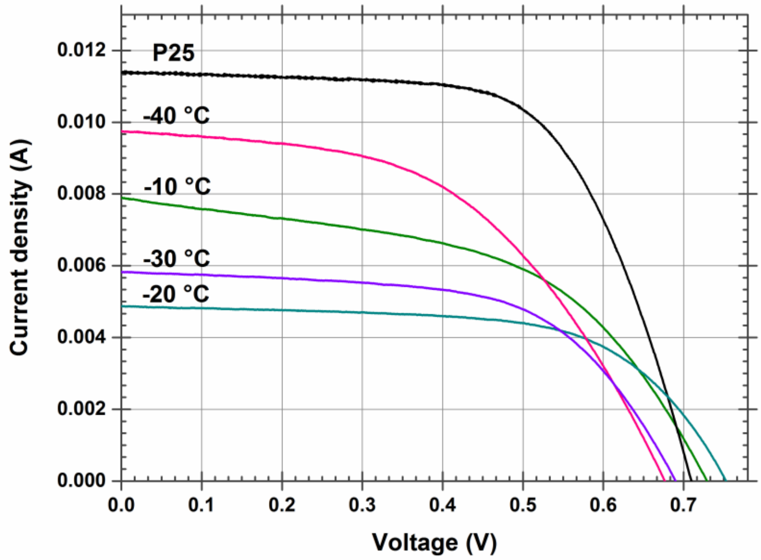

Samples over a range of temperature from -40 °C to -10 °C were synthesized in the reactor and correspondingly their cells were fabricated. Respective current density – voltage graph is plotted as given in figure S1. As temperature decreases the efficiency increases except for -10 °C where a higher efficiency is observed than -30 °C and -20 °C. And, hence -40 °C and -10 °C samples are studied than the rest to design high photoconversion efficient DSSC.

Table A1: Parameters of DSSC fabricated at various conditions

Sample	Anatase Wt. %	Rutile Wt. %	Efficiency
Anatase (See ref. 46 in table S2)	100	0	4.01
Rutile (See ref. 47 table S2)	0	100	3.2
-40 °C	58	42	3.3
-10 °C	27	73	2.9

Figure S2. Williamson Hall plot of both samples to determine the lattice strain, derived from the XRD data of both samples.

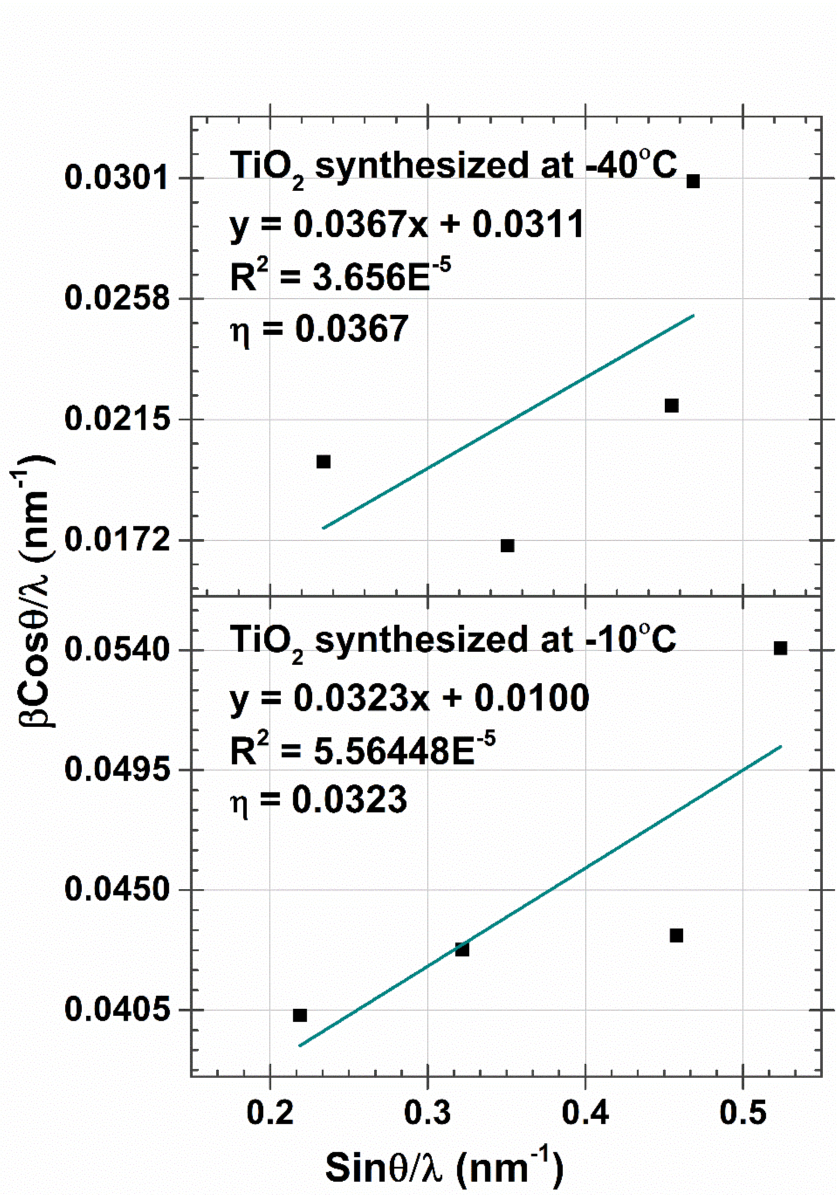

Figure S3. AFM images of the S1, S2 and S3 sample photoanodes.

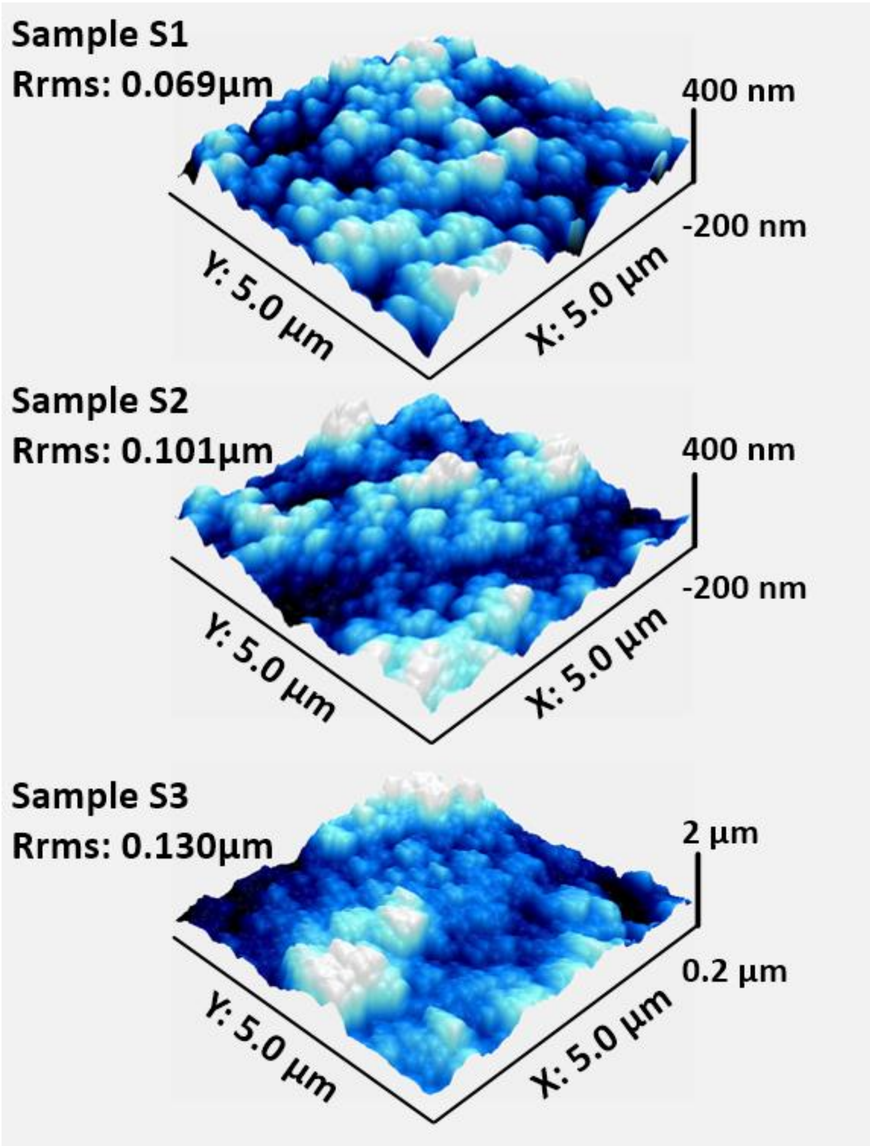

As the concentration of TiO_2 synthesized at -40 °C increases in sample S1 and S2 films, the intensity of the columnar microstructure was decreased as percentage of nanorods declined leading to reduced height of the columnar microstructure with increased size of spherical grains. At the highest concentration, an S3 film consisting of nanocrystals with bigger spherical grain size showed the lowest intensity in the columnar microstructure. The increased -40 °C concentration in compositions enhances roughness along the films and clearly shows improvement in the number of anchoring sites for the dye molecules and electrochemical property of the films.

Figure S4. Dye absorbed amount of S1, S2 and S3 sample photoanodes are calculated using absorption spectra.

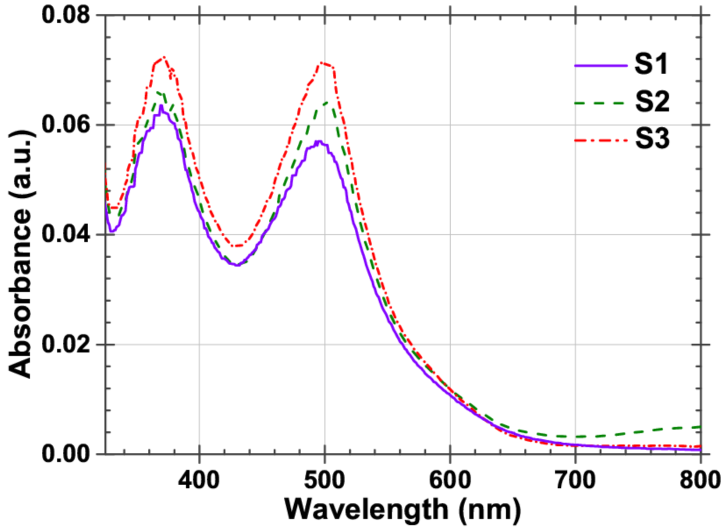

Figure S5. Schematic showing film structures and their respective light scattering.

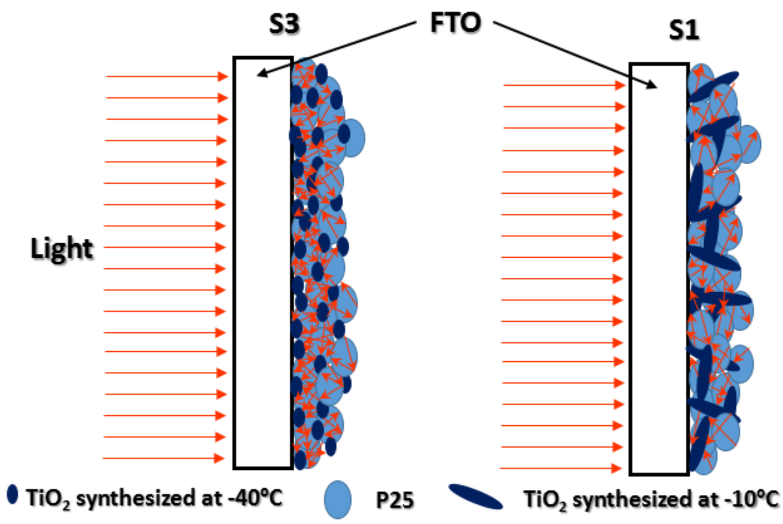

The size of TiO_2 prepared at -40°C was much smaller than that at -10°C. Smaller particles consists of large surface area and together with P25 particles photons from lights have more number of sites to scatter as shown in S1.

Table A2: Literature brief about synthesis of titania at low temperature

Sr. No.	Article	Synthesis Method	Precursor for TiO_2 Synthesis	Low Synthesis Temperature (°C)	Phase
1.	J. Alloys. Compd. 2015, 647,627	Sol-gel method	TTIP	25 to 80	Anatase
2.	Adv. Sci. 2015, 2, 1500070	Wet Condition	TTIP and TiO_2 Nanowire bundles	40	Anatase & rutile
3.	Appl. Surf. Sci. 2015, 355, 1051	Hydrolysis	Tetrabutyl titanate	RT	Anatase
4.	J. Sol-Gel Sci. Technol. 2015, 76, 395	Hydrolysis	Titanium n-butoxide	40 to 70	Anatase, rutile & brookite
5.	PCCP, 2015, 00, 1	Sputtering	TiO_2 crystal	RT	Rutile
6.	Integr. Ferroelectr. 2015, 160 ,142,	Hydrothermal	$Ti(SO_4)_2$	90	Anatase
7.	J. Phys. D: Appl. Phys. 2015, 48, 295201	Sputtering	Ceramic TiO_2 disc	RT to 400	Anatase & rutile
8.	Appl. Surf. Sci. 2015, 04, 125	PLD	TiO_2 pellet	RT to 600	Rutile
9.	RSC Adv., 2015, 5, 45122	Hydrolysis	Tetra-n-butyl titanate	70	Rutile
10.	Chem. Eur. J. 2014, 20, 14763	Hydrothermal	Tetrabutyl titanate	180	Anatase
11.	J. Colloid and Interf. Sci. 2015, 1, 442	Sol-gel method	TTIP	RT	Anatase, rutile & brookite
12.	J. Phys. Chem. B 2005, 109, 8673	Hydrothermal	Tetrabutyl titanate	RT	Anatase & rutile
13.	J. Phys. Chem. C 2007, 111, 2709	Hydrolysis	$TiCl_4$	50	Rutile
14.	J. AM. CHEM. SOC. 2003, 125, 14539	Hydrolysis	TTIP	80	Anatase
15.	J. Mater. Chem. A, 2015, 3, 4477	Sol-gel method	TTIP	50	Anatase
16.	RSC Adv., 2015, 5, 15118	Hydrolysis	$[Ti_8O_{12}(H_2O)_{24}]Cl_8{\cdot}HCl{\cdot}_7H_2O$	RT	Anatase & rutile
17.	Mater. Res. Bull. 2015, 67, 140	Sol-gel method	Tetrabutyl titanate	50 to 90	Anatase
18.	Int. J. Electrochem. Sci. 2014, 9, 3068	Sol-gel method	Tetrabutyl titanate	50	Anatase & brookite
19.	Ferroelectrics, 2013, 457, 30	Hydrothermal	TTIP	100 to 200	Anatase
20.	Environ. Technol. 2014, 35-2, 203	Hydrothermal	Tetrabutyl titanate	100	Anatase & brookite
21.	Cryst. Res. Technol. 2013, 48-11, 969	Sol-gel method	$TiCl_4$	15 to 35	Anatase

22.	Cryst. Growth Des. 2013, 13, 4730	Hydrothermal	TTIP	RT to 200	Rutile
23.	J. Mater. Chem. A, 2013, 1, 8045	Sol-gel method	TTIP	40 to 75	Anatase & rutile
24.	Appl. Catal. B- Environ. 2013, 9, 140	Hydrothermal	TTIP	70	Rutile
25.	Appl Nanosci 2013, 3, 167	Hydrothermal	TTIP	100	Anatase & rutile
26.	Nanoscale, 2013, 5, 2850	Sol-gel method	TTIP	60	Anatase
27.	J. Colloid Interf. Sci. 2013, 90, 396	Sol-gel method	Titanium n-butoxide	80	Anatase
28.	J. Photoch. Photobio. A 2013, 175, 251	Sol-gel method	TTIP	200	Anatase
29.	Materials Letters 2013, 92, 287	Sol-gel method	TTIP	100	Anatase
30	Appl. Surf. Sci. 2013, 265, 317	Sol-gel method	Titanium ethoxide	4	Anatase
31	J. Mater. Chem., 2012, 22, 23906	Hydrothermal	$TiCl_4$	120	Anatase
32.	Electrochimica Acta 2012, 18, 67	Hydrolysis	TTIP	80	-
33.	J. of Mol. Catal. A- Chem. 2011, 97, 335	Hydrolysis	Tetrabutyl titanate	15	Anatase & brookite
34.	J. Photoch. Photobio. A 2010, 201, 216	Sol-gel method	TTIP	RT	Anatase & rutile
35.	J. Cryst. Growth 2007, 179, 304	Sol-gel method	Titanium butoxide	50	Anatase & rutile
36.	Mater. Res. Bull. 2006, 41, 2276	Hydrothermal	TTIP	200	Anatase
37.	Photochem. Photobiol. Sci., 2009, 8, 657	Sol-gel method	TTIP	85	Anatase
38.	J. Phys. Chem. C 2009, 113, 4031	Hydrolysis	Tetrabutyl titanate	40 to 120	Anatase
39.	J Nanopart Res 2008, 10, 233	Sol-gel method	Tetra-n-butyl titanate	103	Anatase
40.	Materials Letters 2008, 62, 4563	Sol-gel method	$TiCl_4$	40	Rutile
41.	Chem. Eng. Technol. 2008, 1277, 31- 9	Hydrolysis	titanyl diacetate & titanyl dibutoxide tetraacetate	60 to 80	Anatase
42.	J. Phys. Chem. of Solids 2008, 69, 1980	Sol-gel method	Tetrabutyl titanate	75	Anatase
43.	Mater. Chem. Phys. 2008, 111, 313	Sol-gel method	Titanium(IV) Sulfate	70	Rutile
44.	J. Colloid Interf. Sci. 2010, 345, 181	Hydrolysis	$TiCl_4$	100	Rutile
45.	J. Phys. Chem. of Solids 2010, 71, 507	Hydrothermal	Titanium(IV) Sulfate	160	Anatase
46	Electrochimica Acta., 2015, 160, 296.	Hydrolysis	Titanium(IV) butoxide	200	100% Anatase

47	Optik, 2016. http://dx.doi.org/10.1016/j.ijleo.2016.01.034	Hydrothermal	Titanium(IV) butoxide	150	100% Rutile
48.	Our study	Sol-gel method	TTIP	-40 and -10	Anatase & rutile

RT=Room Temperature